ELSEVIER

Nuclear Instruments and Methods in Physics Research A 439 (2000) 427–441

NUCLEAR INSTRUMENTS & METHODS IN PHYSICS RESEARCH Section A

www.elsevier.nl/locate/nima

Design and test of radiation hard p^+n silicon strip detectors for the ATLAS SCT

L. Andricek[a,*], D. Hauff[a], J. Kemmer[b], E. Koffeman[a], P. Lükewille[a], G. Lutz[a], H.G. Moser[a], R.H. Richter[a], T. Rohe[a], H. Soltau[b], A. Viehl[b]

[a]*Max-Planck-Institut für Physik, Werner-Heisenberg Institut, Fohringer Ring 6, Postfach 401212, 80805 München, Germany*

[b]*KETEK GmbH Oberschleissheim, Germany*

Abstract

Strip detectors covering radiation hardness and large-scale production ability are developed and produced for the ATLAS experiment at the Large Hadron Collider (LHC) at CERN (Switzerland). Capacitively coupled p^+n detectors (p-type strips on n-type substrate) were developed with implanted bias resistors in order to simplify the detector processing addressing the requirements of large-scale production. The detectors were irradiated with 24 GeV protons up to $3 \times 10^{14}\,\mathrm{cm}^{-2}$ in order to simulate a 10 years operation scenario at LHC. The presented static and signal measurements demonstrate the function of the device concept before and after irradiation. © 2000 Elsevier Science B.V. All rights reserved.

Keywords: Silicon detectors; Radiation hardness; Implanted resistors

1. Introduction

The detectors to be described in this paper have been developed at the MPI Semiconductor Laboratory for use in the ATLAS experiment at LHC. Concept and design are based on earlier experience with double sided detectors [1] and extensive device simulations. A p^+n option (p-type strips on n-type substrate) has been chosen for reasons of simplicity of the production method. Simultaneously the lower electrical field strengths make these devices less prone to impact ionization and electrical breakdown. The detectors designed for LHC operation will have to function properly despite the drastic radiation-induced material property changes, in particular it should be possible to operate them at least 350 V, the operation voltage specified for ATLAS. The harsh radiation environment is the main challenge for strip detectors operated at LHC experiments. For example, the innermost barrel layer of the ATLAS SCT (SemiConductor Tracker) has to withstand a radiation dose of $2 \times 10^{14}\,\mathrm{cm}^{-2}$ 1 MeV equivalent neutrons [2]. In addition they should be tolerant to local defects in the production process, allow potential individual problems to be spotted before irradiation, and require a simple technology so that they can be produced at low cost.

Capacitively coupled detectors are used in ATLAS in order to decouple the amplifier inputs from the detector leakage current thereby avoiding channel-to-channel and time-dependent pedestal shifts.

* Corresponding author. Tel.: +49-89-83940055.
E-mail address: ladislav.andricek@cern.ch (L. Andricek)

0168-9002/00/$ - see front matter © 2000 Elsevier Science B.V. All rights reserved.
PII: S0168-9002(99)00901-8

To realize the bias resistors usually polysilicon is used which is a cost driving process. We replaced this technology by simple implanted resistors.

2. Detector design and technology

Exposing detectors to the radiation environment at LHC will induce bulk defects with concentrations exceeding by far those of the original dopants. In addition oxide and Si–SiO_2 interface damage leads to an order of magnitude increase of the oxide charge. The well-known consequences of the bulk material changes [18] are an increase of detector leakage current, the change of effective doping from n- to p-type (type inversion) followed by a steady increase of full depletion voltage, and signal loss due to enhanced charge trapping after radiation damage.

Also very relevant for the operation of heavily irradiated detectors is the low conductivity of the undepleted bulk material found experimentally [3–5] which can be explained by the creation of near mid gap acceptor-type defects [6]. It gives a key for understanding the survival of single sided p^+n detectors after type inversion even if the pn-junction moves towards the cutting edge [7].

At the silicon/silicondioxide interface the radiation induced increase of oxide charge can lead to locally enhanced electric field strengths and, as a consequence, to electric breakthrough and micro-discharges.

2.1. *Breakdown prevention*

The main issue is the required high-voltage stability. The projected maximum operation voltage in ATLAS SCT is 350 V after 10 years of operation. A reduction of high electric fields within the device improves the survivability of the detectors in the experiment as well as the production yield. Two ways to achieve this are the implementation of break down protection structures for the edge region [8] and the use of drive in diffusion steps leading to smoother junctions and lower electric fields. Another technological measure widely used in microelectronics to reduce high field effects in short channel MOS transistors is the implementation of the so-called ligthly doped drain (LDD) structures [9]. High electric fields at the drain of typically n-channel devices are suppressed by implantation of low-doped extensions overlapping the actual n^+ regions. A similar structure can be introduced in detector technologies by extending the strip edges by a low-dose implantation.

2.1.1. *Multi-guard ring structures*

Avalanche breakdown caused by impact ionization due to accelerated charge carriers in high electric fields as well as punch through currents crossing potential barriers between neighboring p^+ guard rings may lead to a signifcant current increase with raising voltages.

Considering neighboring guard rings a small guard distance leads to low electric fields but also to low potential barriers between the rings resulting in an early onset of the punch through current. For large gaps the relations are inverted. In the design punch through and impact mechanisms have to be balanced in order to combine high-voltage blocking capability with modest space consumption and relaxed design rules. However, a moderate onset of punch through current is preferred to high fields and resulting avalanche breakdown which is usually attributed with noise and hot electron-induced damage of the oxide layers.

The potential of the guard rings is adjusted by the punch through current. The potential barrier between two rings depends on the gap between the p^+ rings, the detector bias voltage, the leakage current itself, the doping density, the oxide charge, the oxide thickness and the potential on top of the oxide. The latter one can be defined by metal overlaps contacted to the inner or the outer p^+ neighbor. The oxide charge density, the bulk doping and leakage current are strongly influenced by irradiation. Ionizing radiation causes an increase of the fixed positive oxide charge saturating at a level of an order of magnitude higher than the initial one. Thus, the risk of micro-discharges or electric break down is increased, particularly at locations where crystal defects like dislocations or oxygen precipitates are present. However, any field reduction introduced by technological means or via design increases the yield in terms of break down stability. While the effect of increasing oxide charges is

measured and modeled in [10] using Gamma irradiation, a detailed understanding of the influence of radiation-induced type inversion on the multi guard structures has not yet been achieved. A key mechanism is the high ohmic bulk resistance if operated at or near to equilibrium which is caused by the creation of deep acceptor levels during irradiation [4–6] but the potential distribution within an irradiated guard structure cannot be explained by this phenomenon alone.

We use a guard structure with 16 rings divided in two regions Fig. 1. An inner one with relative small gaps between the rings prevents impact ionization. The highest electric field of the whole guard structure is on the outer edge of the bias ring at the interface to the oxide. This is the reason why the gap between the bias ring and the first guard ring was chosen as the smallest one in the whole structure (6 μm).

The outer part of the guard structure have rather large gaps increasing the punch through voltage between the rings in this region. This allows also a resistive voltage drop after irradiation when deep level acceptor states dominate the device behavior. Wide inward metal overlaps define a relative positive potential at the $Si–SiO_2$ interface beneath it keeping electrons there and suppressing punch through of holes between the rings.

Fig. 2 shows the potential of a sample of guard rings surrounding a $5 \times 5\,mm^2$ diode up to a bias voltage of 500 V. The structure was irradiated by 24 GeV protons ($2 \times 10^{14}\,cm^{-2}$). These measurements were performed on a probe station at room temperature.

The moderate voltage drops between the rings indicate that the structure operates satisfactorily after irradiation.

2.1.2. Reduction of electric fields in the strip region

The highest electric fields in the sensitive region of the device are located at the lateral edge of the p^+ implantation due to the presence of fixed positive oxide charge N_{ox}. This is in the range of $2 \times 10^{11}\,cm^{-2}$ for a high quality oxide grown on $\langle 1\,1\,1 \rangle$ oriented silicon. Reducing the doping density at the strip edge in contact with the accumulation layer also reduces the electric field and therefore the tendency of avalanche break down. To achieve this no additional processing steps are needed. The structures are integrated into the nitride opening mask. The boron implantation for the bias resistors (see below) is used to dope the graded strip extensions.

Fig. 3 shows a two-dimensional doping profile illustrating the doping distributions of a lightly doped strip (LDS) structure resulting from overlapping

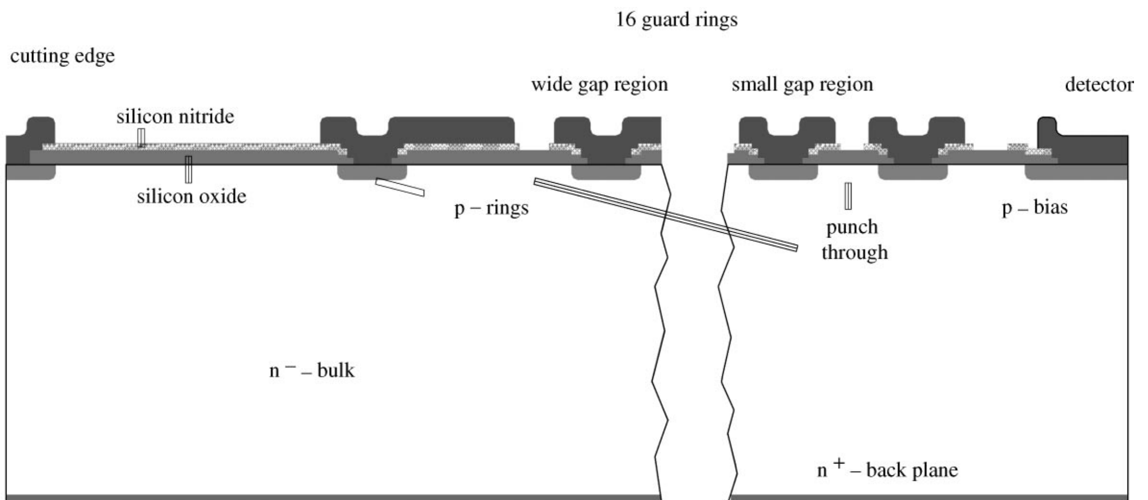

Fig. 1. Simplified cross section of a p^+n detector with multi-guard ring structure with 16 rings.

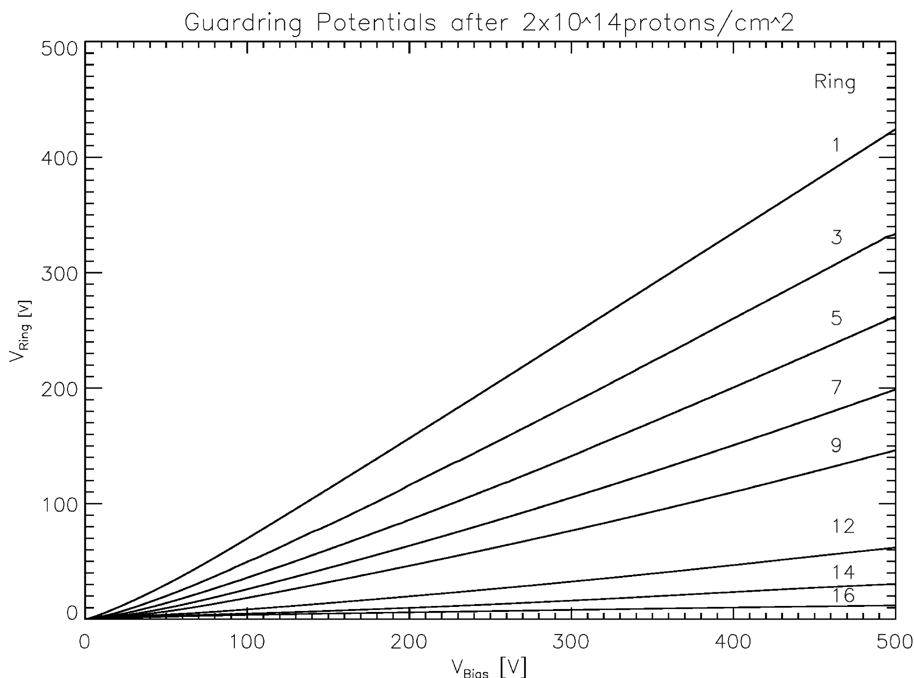

Fig. 2. Guard potentials surrounding a 5×5 mm^2 diode after a proton irradiation (24 GeV) of 2×10^{14} cm^{-2}, measured at 20°C.

strip implants with the resisitor implants. This structure is layed out as a frame surrounding each individual strip. A field reduction of 20% is calculated by two-dimensional device simulation as shown in Fig. 4 assuming an oxide charge density of 1.5×10^{12} cm^{-2}. The results were obtained using the technology simulator DIOS [11] and the device simulation program ToSCA [12].

2.2. Bias resistors

2.2.1. Resistor values required for LHC

The resistance value of the bias resistor is determined by the requirement that the contributed additional noise is negligible compared to the total noise of the system. Following [2] the detector noise (mainly dominated by the front end amplifier with connected strip capacitors) is about 1500 e$^-$. During irradiation this number will be increased further by degrading detector and electronics properties. The bias resistor on the detector, located parallel to the amplifier input, will contribute a noise charge of

$$\mathrm{ENC}_{R_{\mathrm{bias}}}(\mathrm{e}^-) = \frac{1}{q}\sqrt{\frac{4kT\tau_{\mathrm{f}}}{R}}$$

to the signal. In this simplified expression for the thermal noise k is the Boltzmann constant, τ_{f} the signal formation time (20 ns), T the absolute temperature, and q the elementary charge. It is added in quadrature to the noise of all other sources ENC_0. Fig. 5 visualizes this dependence of the total noise charge on the resistance value with the noise of all other sources ENC_0 as parameter. It demonstrates that a resistor value above hundred kΩ already adds negligible noise when using fast ATLAS read-out electronics.

2.2.2. Implanted or polysilicon resistors

Implanted resistors are widely used in all kinds of microelectronic circuits. They are well known for their reproducibility especially in the low and medium resistance range. In contrast to polysilicon

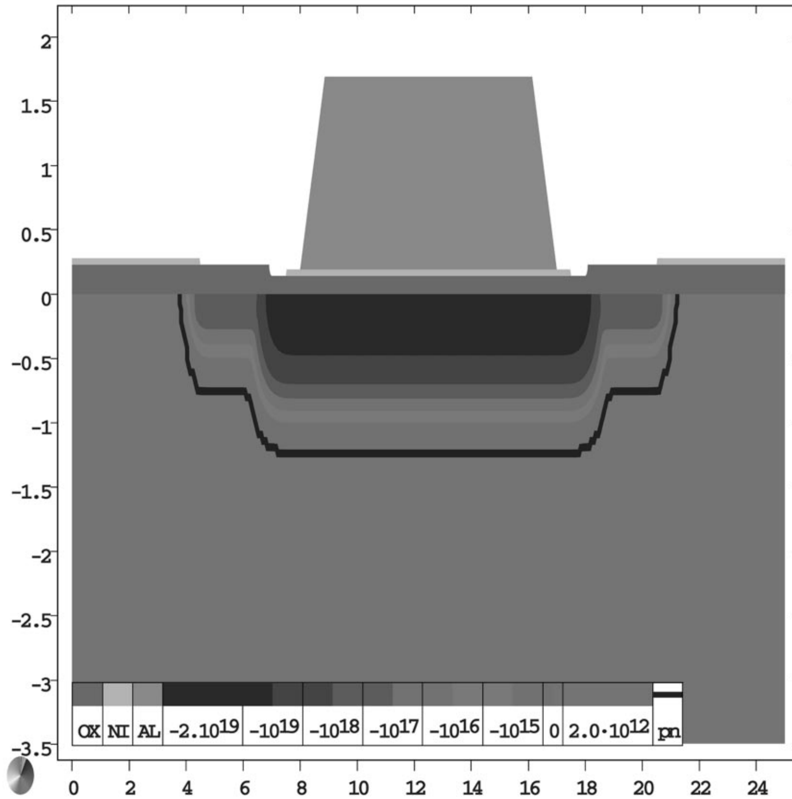

Fig. 3. Two-dimensional doping simulation of the strip cross section with low doped strip extensions (x–y dimensions are given in microns).

resistors, which need an extra film on top of the SiO_2, implanted resistors consist of an ion implanted region within the silicon itself Fig. 6.

Besides the chemical vapor deposition and etching of polysilicon, most polysilicon processes optimized for resistors in the required range need in addition two implantations, one for the resistance definition itself and another high dose one to provide an ohmic contact system to the metal. To define the polysilicon pattern and the mentioned contact regions two lithographic steps are needed, while the implanted resistor option needs one implantation and at most one lithographic step.[1]

[1] By an appropriate integration into the entire detector process this masking step can even be saved (see below).

The additional effort compared to the implanted resistor technology causes not only a significant price increase but introduces also additional sources of possible failures, thus requiring more elaborate acceptance tests.

Because of the large contact openings in the guard and bias regions the yield of a typical strip detector technology is not sensitive to technological contact problems like incomplete contact openings or interfacial layers. While implanted resistors do not need any additional contacts, polysilicon resistors require either a silicon/polysilicon via contact system or a metal bridge system connecting p^+ regions of the monocrystalline silicon to those of the polysilicon.

Both kinds of contact devices may affect the detector yield. The polysilicon resistance is not only

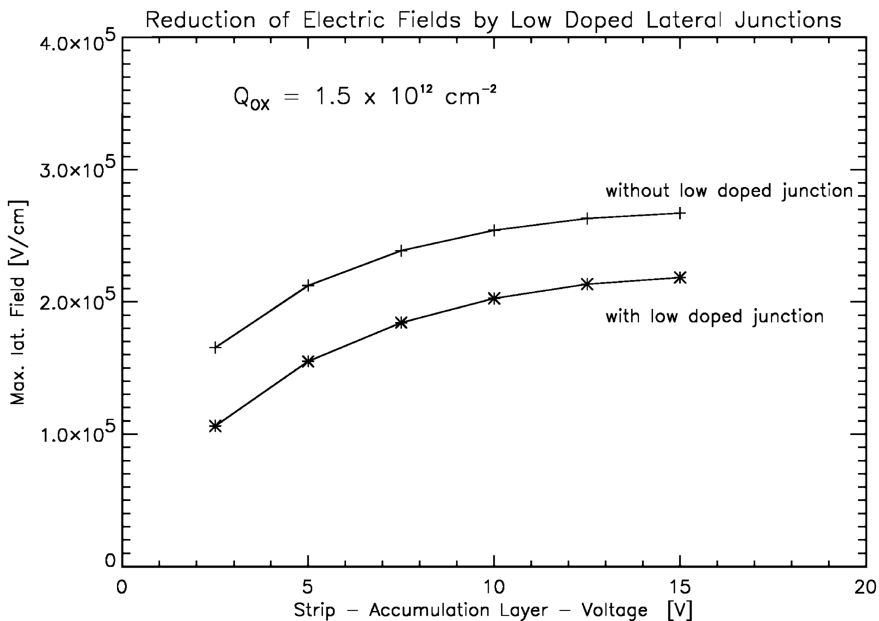

Fig. 4. Simulated maximum electric field with and without lightly doped strip extensions.

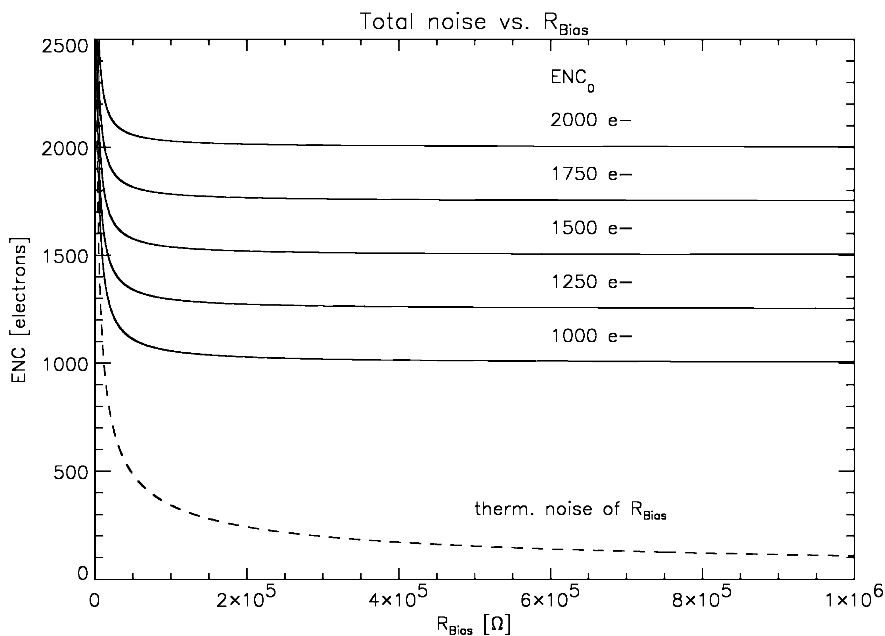

Fig. 5. Contribution of the bias resistor to the total noise for different initial noise levels (electronics + detector) under ATLAS SCT conditions. The total noise is shown as function of the bias resistance.

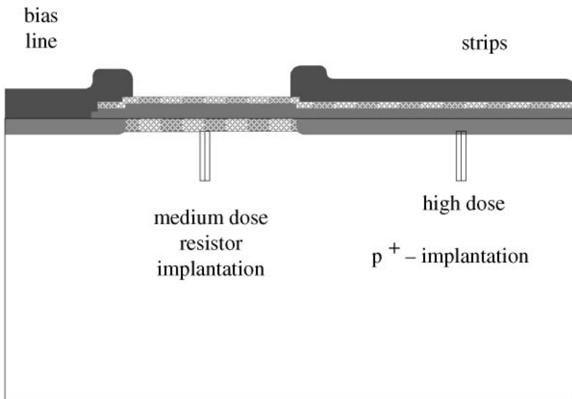

Fig. 6 . Simple process integration of p doped implanted resistors in a p-on-n strip detector. Contacts are not necessary.

defined by the implantation dose but also by the polysilicon grain size. The exponential dependence of resistance vs. film thickness [13] results in bad reproducibility of the resistance value, in particular when comparing different production batches.

2.2.3. Implantation parameters

Implementing implanted resistors in the detector technology the lower limit of the resistance value is given by tolerable thermal noise contribution while the upper limit is set by safety aspects concerned with the radiation-induced degradation of the silicon and SiO_2, and the space available in the detector design. The negative boron acceptors of the resistor implantation will be partially compensated by radiation-induced positive oxide charges leading to an increasing bias resistance. However, as long as the resistor channel is not pinched off, an increasing bias resistance does not affect the noise performance of the detector. Dimensioning the resistor implantation dose one has to take into account that the generated fixed oxide charge has to be compensated by an acceptor charge of the resistor. Hence, pinch off is avoided if the implanted acceptor dose is substantially larger than the sum of all effective positive oxide charges.

Most of the electron–hole pairs in SiO_2 generated by ionizing radiation recombine immediately, only a fraction is separated. While electrons in SiO_2 have high mobility and escape relatively fast, holes are extremely slow and may be permanently captured in deep level traps of the oxide particularly in the Si/SiO_2 transition region [14]. Thus positive charge accumulated is in the oxide and in the oxide–semiconductor interface leading to threshold shifts in MOSFETs and high field regions in the detector. A saturation of the radiation-induced oxide charge is observed which may be explained by the limited number of available traps [14,15]. An effective Boron implantion dose of $10^{13}\,\mathrm{cm}^{-2}$ was chosen for the detector prototyping for the ATLAS-SCT Forward Region. A one-dimensional simulation [11] of the doping profile is shown in Fig. 7. The calculated sheet resistance is $2.9\,\mathrm{k\Omega/sq}$ (Fig. 8).

2.2.4. Irradiation of implanted resistors

The irradiated detectors were biased via implanted resistors and the S/N measurements (see Section 3) show that there is no unacceptable noise after irradiation with the full anticipated dose after 10 years LHC operation. The resistance values were tested before and after irradiation and an increase of about 20% was found after irradiation.

Separate test structures made by CiS, Germany (together with full size ATLAS-SCT detectors for the forward region) were irradiated with X-rays from a tungsten target (energy continuum with a peak at 10 keV). The irradition was carried out on an X-ray irradiation facility at CERN. There are five resistors per test structure with different aspect ratios. The implantation dose for the resistors resulted in a sheet resistance before irradiation of $3\,\mathrm{k\Omega/sq}$ and, according to the various aspect ratios, in a total resistance between 30 and 220 kΩ. The resistors were not biased during the irradiation and the resistance was measured by applying 1 V across the resistor and recording the current. The IV characteristics in the range between -1 and $+1$ V had a perfectly linear behavior both before and after irradiation. Five test structures each of them with five resistors were measured after different doses. Fig. 9 shows the result for one structure. As expected the resistance increased after irradiation due to the higher concentration of trapped charges in the oxide/nitride layer. All of the devices had a similar behavior and the relative change of the resistance is in the range between 15% and 24% for all resistors (Fig. 10).

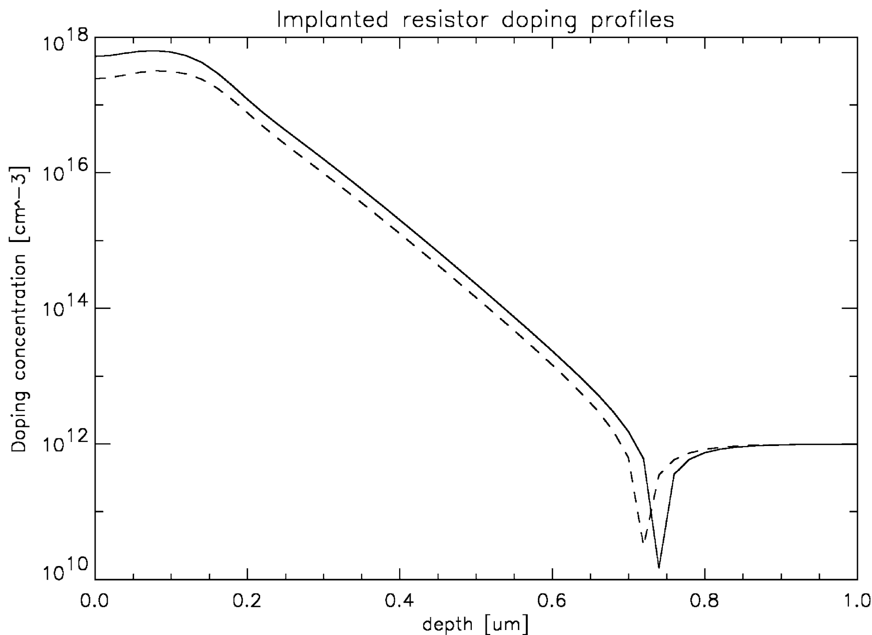

Fig. 7. Simulated doping profiles of the resistor implants with effective boron doses of (A) $5.3\times10^{12}\,\mathrm{cm}^{-2}$ (dashed line) and (B) $10^{13}\,\mathrm{cm}^{-2}$ (solid line), respectively.

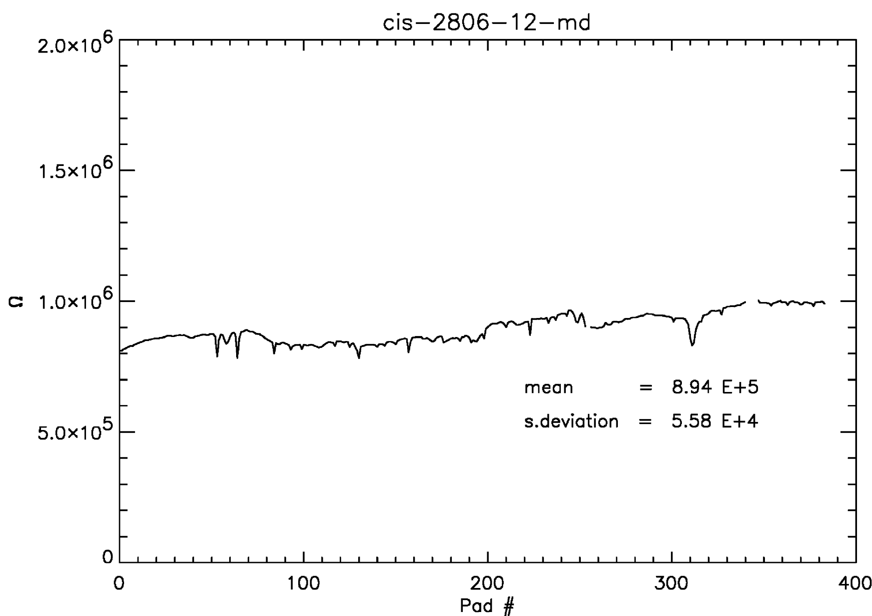

Fig. 8. Resistance variation across prototype detector CiS 2806-12.

A sample of 32 meander-type resistors from two other CiS batches with the same implantation dose and energy were tested separately up to a dose of 10 Mrad, the expected dose after 10 years LHC operation. The mean value of the resistance increased by 18% (Fig. 11).

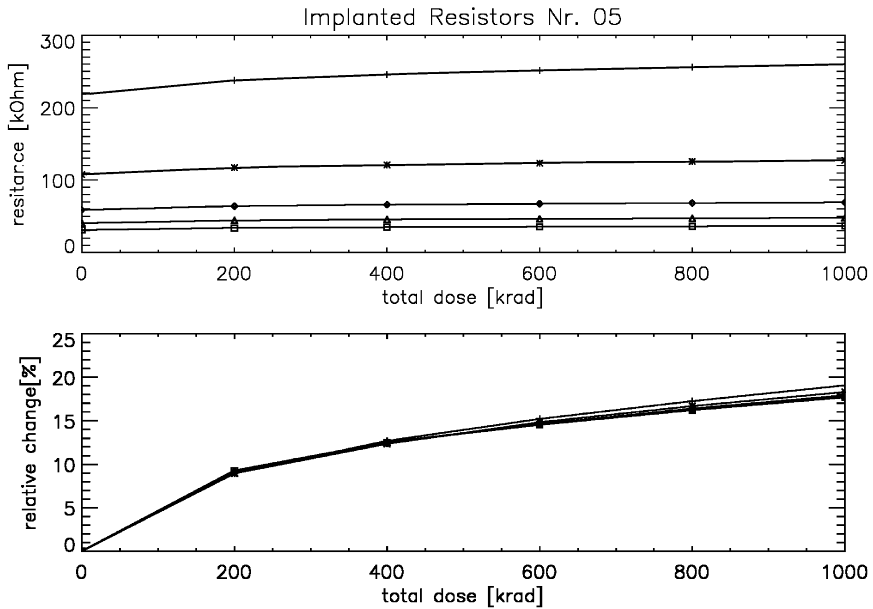

Fig. 9. Total resistance and the relative change of implated resistors due to irradiation with X-rays up to a dose of 1 Mrad.

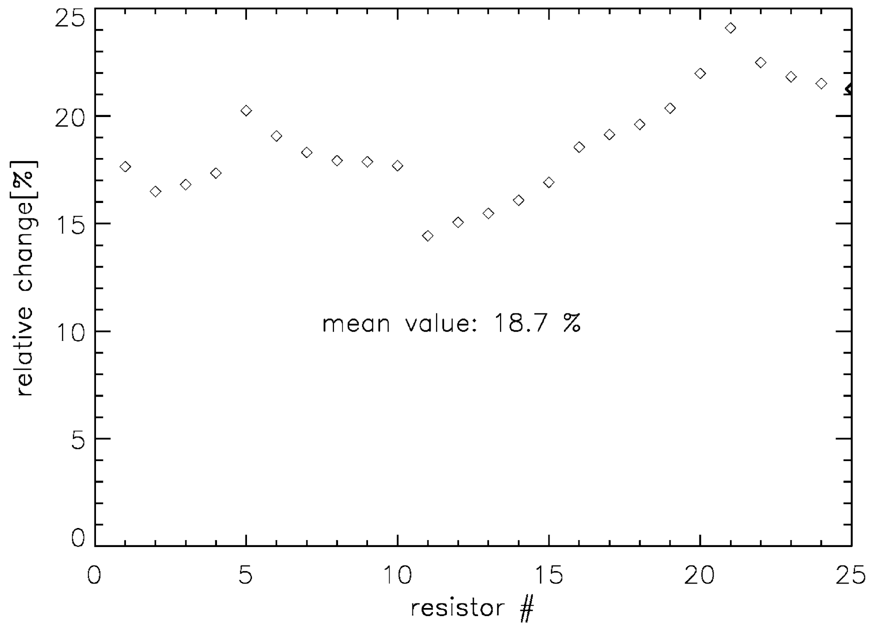

Fig. 10. Increase of the resistance after irradiation with 1 Mrad. 25 implanted resistors were tested, on the average the resistance increased by 18.7%.

2.3. Safety feature

The layout of the biasing region in Fig. 13 shows another interesting feature. There is a punch-through structure in parallel to the bias resistor. In normal operation mode the voltage drop across the bias resistor is too small to turn on the punch through between bias line and strip. But in the case

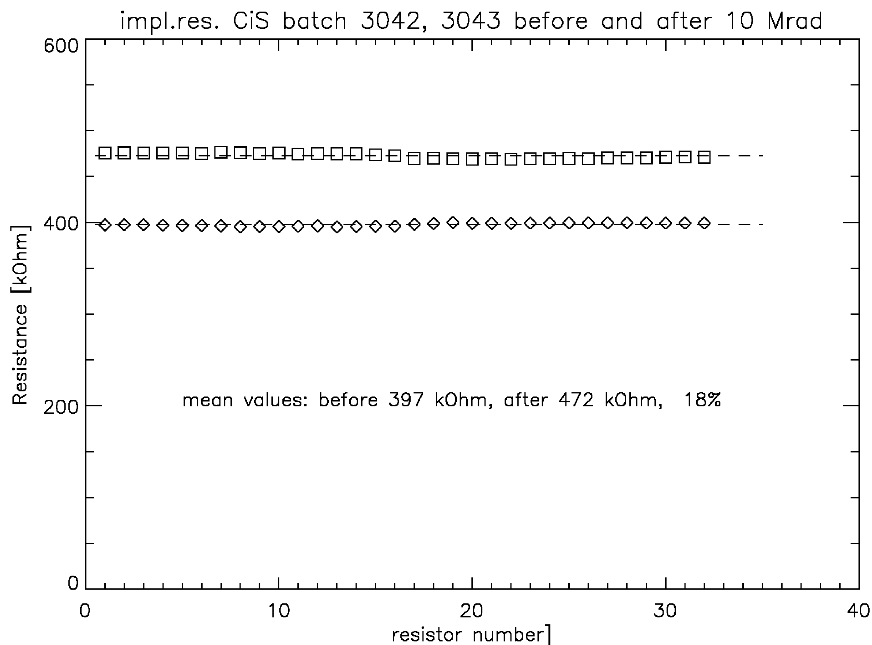

Fig. 11. After 10 Mrad X-ray irradiation the mean resistance value of 32 tested resistors increased by 18%.

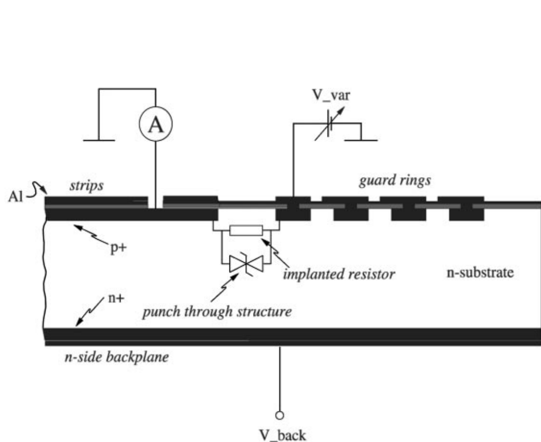

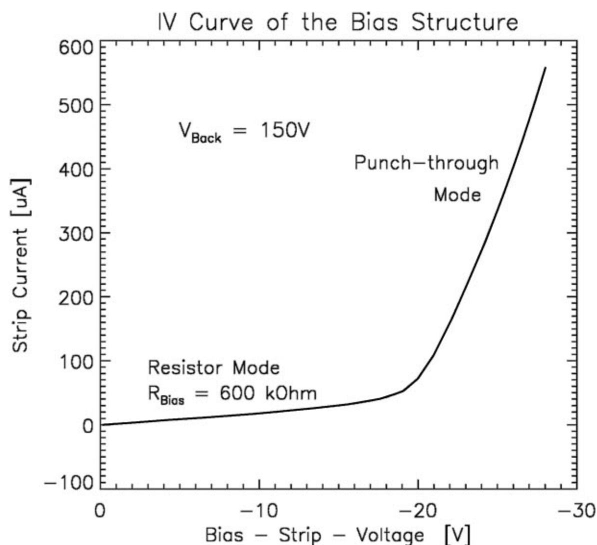

Fig. 12 . Onset of the parallel punch-through structure is around 20 V. A high current of around 0.5 mA due to a sudden radiation burst would result in a voltage drop between strip metal and implant of only 27 V.

of a sudden radiation burst the resulting high strip current is drained by this punch through structure instead of the bias resistor. The aim is to prevent large voltage across the strip dielectrics. The measurement result in Fig. 12 shows that the onset of the parallel punch-through structure is around 20 V.

A high current of around 0.2 mA due to a sudden radiation burst results in a voltage drop between strip metal and implant of only 23 V. The voltage drop along the strip implantation is neglected in this measurement.

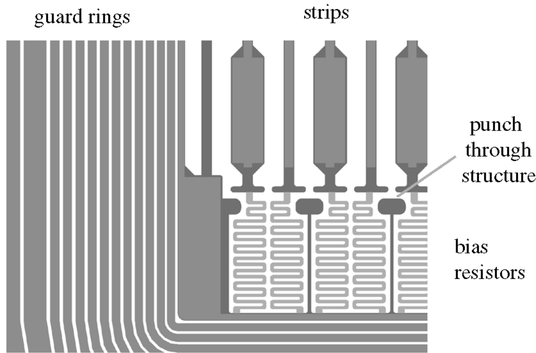

Fig. 13. Closeup of the detector edge region including strip bias resistors and multiguard edge protection structure. The punch-through structure operating in parallel to the resistor limits the voltage drop across the resistor in case of irradiation bursts.

2.4. Processing

To take full advantage of the p^+n detector choice a technology has been developed which combines high strip yield and large break down voltage with cost effectiveness and reliable operation after irradiation.

A five mask process sequence was used including P^+ strip definition (mask I), resistor definition (mask II), contact openings (mask III), aluminization (mask IV) and passivation (mask V).

In order to avoid shorts between metal and implanted strips a SiO_2/Si_3N_4 sandwich layer is used and structured in two steps using different masks (II and III).

A significant process simplification is achieved by the simultaneous use of the nitride mask for the definition of the implanted resistors. Making use of this simplification resistors have to be implanted through the SiO_2/Si_3N_4 sandwich layer.

A prototype batch was processed on $\langle 1\,1\,1 \rangle$ double-sided polished substrates provided by Wacker Chemitronic. The specified bulk resistivity

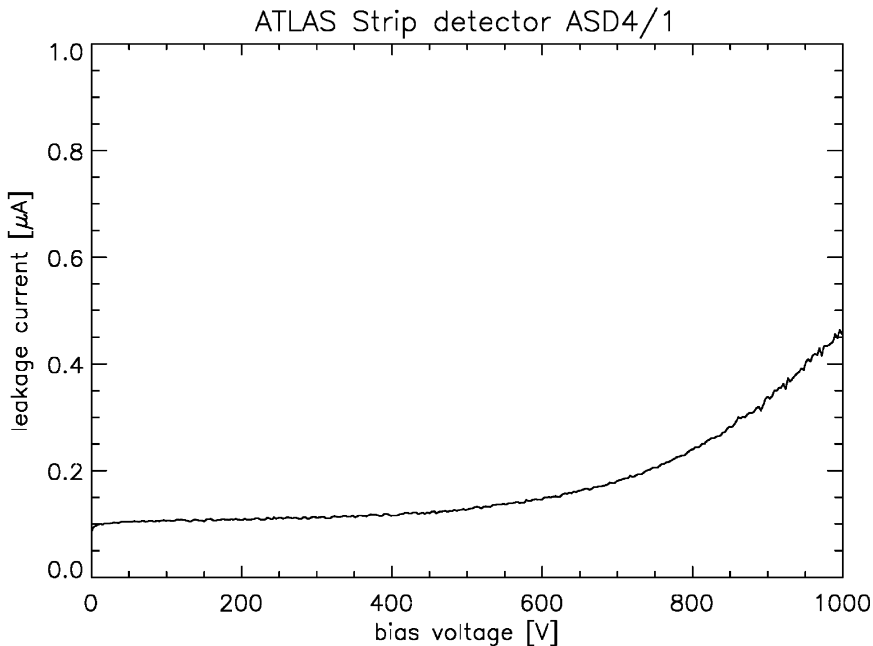

Fig. 14. Current–voltage characteristics of an unirradiated strip detector.

is 2–3 kΩ cm resulting in a depletion voltage range of 80–120 V for 280 μm thick wafers.

3. Detector test results

3.1. Static measurements before and after irradiation

In Fig. 14 the current–voltage characteristic of a full size ATLAS-SCT detector with an active area of roughly $36\,cm^2$. The currents were measured at room temperature up to a bias voltage of 1000 V. No indication of avalanche breakdown was observed.

In September 1997 two detectors fabricated at the MPI Semiconductor Laboratory, and two from commercial suppliers using the same technology were irradiated up to $3 \times 10^{14}\,cm^{-2}$ 24 GeV/*c* protons at the CERN PS. The detectors were biased at 150 V during the irradiation and kept cold at $-7°C$. Subsequent controlled annealing for 21 days at 25°C [16] simulates the yearly warm-up of 2 days at 20°C and 14 days 17°C during 10 years LHC operation in ATLAS [2].

Current–voltage measurements were taken at various temperatures inside a temperature cabinet. The electronics was biased during the measurement and the strips with no readout were held on ground potential by bonding them via the pitch adaptor to a ground line. The temperature of the detector was measured with a thermo-sensor (PT100) placed directly on the detector ceramics. The ceramics are

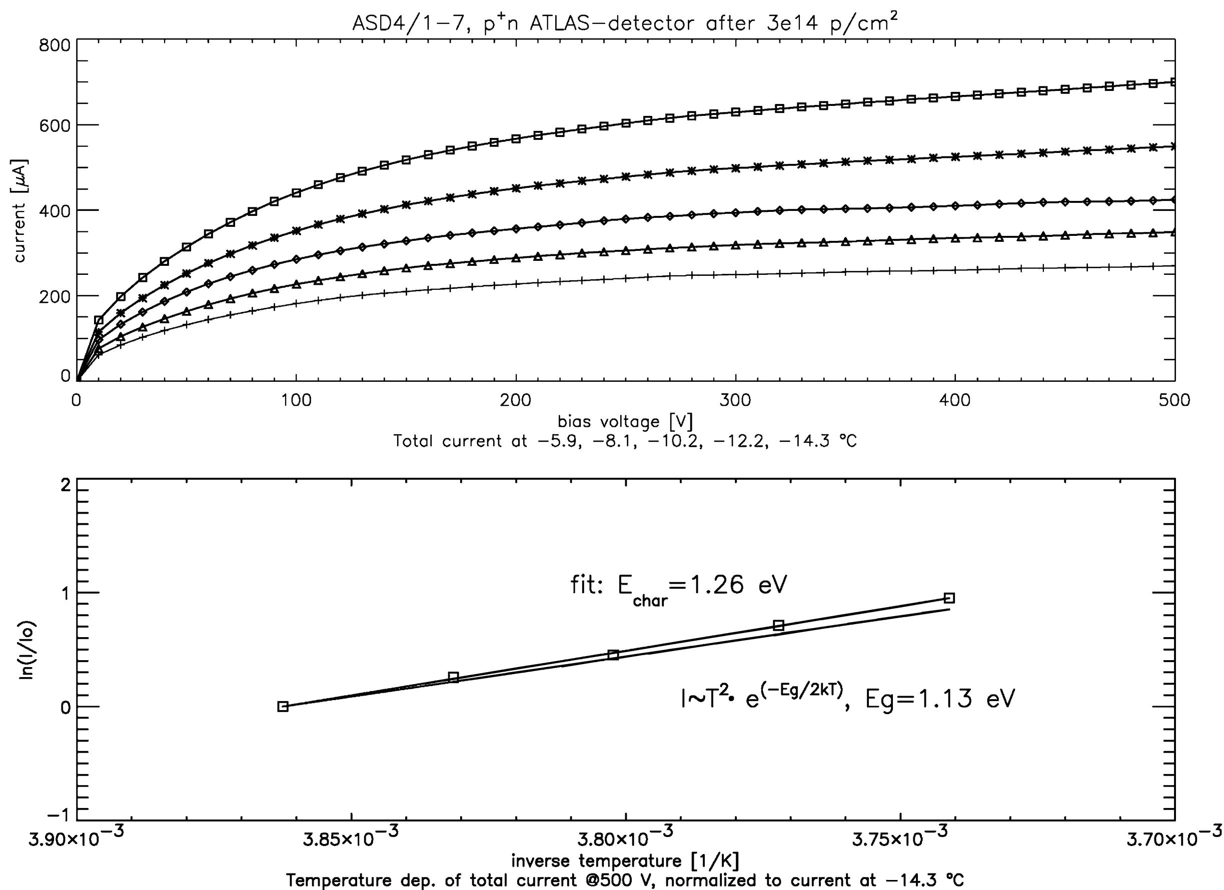

Fig. 15. *IV* characteristics after irradiation and annealing taken at various temperatures.

mounted in an aluminium box, a good cooling of the detector is provided by a strong fan inside the temperature cabinet. No evidence of self heating was observed. Measurements were done at -5.9, -8.1, -10.2, -12.2 and -14.3°C. The temperature dependence of the current at 500 V shows an exponential behavior. But a fit to the curve gives a characteristic energy of 1.26 eV (instead of 1.13 eV band gap at this temperature). This behavior can be understood if one assumes a higher density of traps close to the midgap energy [7] (Fig. 15).

The currents were normalized to 0°C using the standard temperature dependence with the characteristic energy of 1.26 eV. The power desity versus the operating voltage in Fig. 16 shows a linear behavior above a few tens of volt and is roughly 100 $\mu W/mm^2$ at 350 V. After the irradiation also a pinhole test on the strips was performed with an applied voltage of 50 V across the dielectric layers. The strips were correctly biased via the implanted resistors and the punch through structure in parallel during irradiation. No pinholes/shorts were found among the 384 tested strips.

3.2. Signal and noise measurements after irradiation

Signal and noise properties were investigated with unirradiated FELIX electronics [17] which was bonded to the detectors after the end of irradiation. This electronics has an intrinsic risetime of approximately 75 ns and a built in feature of signal processing (deconvolution) making it possible to use effectively 25 ns shaping. Strips were connected in such a way as to study the situation with 6 cm long strips corresponding to the use of a single detector and 12 cm length corresponding to daisy chained detectors as foreseen for ATLAS modules. Signal measurements were performed with a ^{90}Sr beta source.

The signals are reconstructed forming a cluster containing the total charge in a maximum of five consecutive strips. Such a cluster is initiated by a seed of a strip with 4σ signal and accepted when it has a total charge of at least five sigma above the average noise of the particular channels. A Landau distribution (convoluted with a Gaussian) is fitted to the obtained pulse height spectrum.

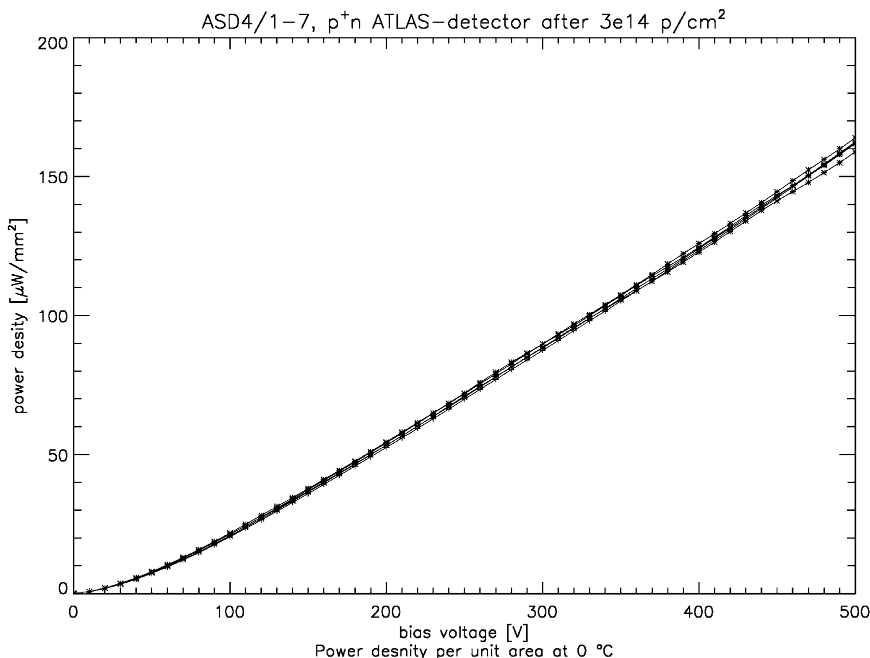

Fig. 16. Power density of the irradiated detector measured at various temperatures and normalized to 0°C.

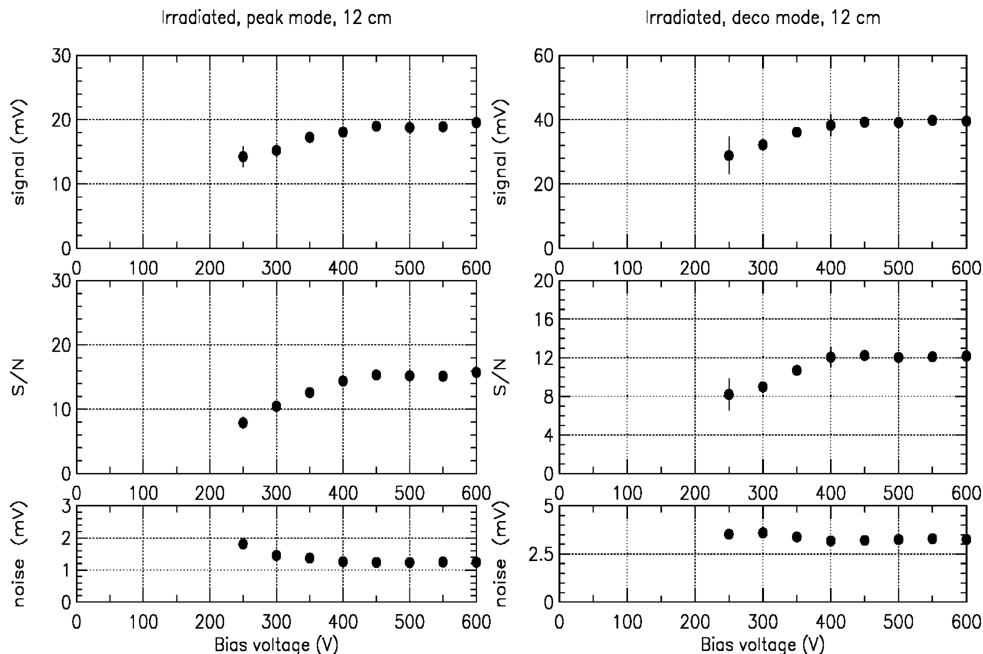

Fig. 17. Signal and noise versus the bias voltage at $-15°C$.

Signal and noise spectra obtained in "peak mode" corresponding to 75 ns shaping are shown as function of the bias voltage in Fig. 17 on the left-hand side. Full signal height on the annealed detector is reached at 400 V, measurements extend up to 600 V. The S/N ratio in the saturation region is 16 for the 12 cm region. Note that the noise does not increase with overdepletion of the detector. Essentially, the same properties are found with 25 ns effective shaping (deconvoluted mode). The corresponding S/N ratio with the ATLAS relevant peaking time is 12 for 12 cm long strips.

4. Summary

Single-sided p^+n strip detectors designed for operation in harsh radiation environments are presented. The use of implanted bias resistors instead of polysilicon resistors leads to a simplified technological process with five masks allowing a cost effective mass production.

In particular, emphasis was put on high-voltage operation which is ensured by reducing the electrical field strengths in both the edge and the sensitive region. A multi-guard ring structure is used for edge protection. The reduction of the electrical fields in the sensitive region is done by reducing the doping density at the strip edges making use of the medium dose implantion for the implanted bias resistors. The new biasing method can be realized with little technological effort compared with the commonly used polysilicon technology. Implanted bias resistors have been irradiated separately in order to investigate the increase in resistivity after exposure to ionizing radiation. After 10 Mrad, the expected dose after 10 years operation in ATLAS, the resistivity changed by a tolarable value of about 20%.

Full size detectors for ATLAS SCT have been produced in the MPI Semiconductor Laboratory and tested before and after irradiation with 24 GeV protons. The detectors are fully operational after a fluence of $3 \times 10^{14}\,cm^{-2}$. At 350 V a signal-to-noise ratio of about 10 : 1 was measured with a FELIX chip operated in the LHC relevant 25 ns read out mode. For these conditions signal saturation was observed at 400 V. Both the current–voltage

characteristics and the noise performance are stable up to bias voltages of at least 600 V.

Acknowledgements

We are indebted to the staff of the semiconductor laboratory who contributed to the production of the detectors and to our colleagues of the ATLAS collaboration who provided help in many aspects and in particular carried the burden of the PS irradiation test. We are grateful to Ogmundur Runolfsson for performing the detector bonding. We also would like to thank Frederico Faccio who kindly made the X-ray irradiation facility available to us.

References

[1] L. Andricek et al., Nucl. Instr. and Meth. A 409 (1998) 184.
[2] ATLAS Inner Detector Technical Design Report, 1997.
[3] I. Tsveybak et al., IEEE Trans. Nucl. Sci. NS-39 (6) (1992) 1720.
[4] Z. Li, Nucl. Instr. and Meth. A 342 (1994) 105.
[5] R. Wunstorf et al., Nucl. Instr. and Meth. A 377 (1996) 228.
[6] G. Lutz, Nucl. Instr. and Meth. A 377 (1996) 234.
[7] G. Lutz et al., Survival of single sided n-bulk detectors after type inversion, Second Workshop on Radiation Hardening of Silicon Detectors, CERN 4–5 February 1997.
[8] A. Bischoff et al., Nucl. Instr. and Meth. A 326 (1993) 27.
[9] S. Ogura et al., IEEE Trans. Electron Dev. ED-27 (1980) 1359.
[10] B.S. Avset, L. Evenson, Nucl. Instr. and Meth. A 377 (1996) 397.
[11] N. Strecker et al., DIOS users guide, Swiss Federal Institute of Technology, Zürich, Switzerland, 1995.
[12] H. Gajewski et al., TOSCA – Two Dimensional Semiconductor Analysis Package, Handbuch, WIAS, Berlin.
[13] N.C.C. Lu, J. Electrochem. Soc.: Solid-State Sci. Technol. 131 (4) (1984) 897.
[14] E.H. Nicollian, J.R. Brews, MOS (Metal Oxide Semiconductors) Physics and Technology, Wiley, New York, 1982.
[15] D.J. DiMaria, D. Arnold, E. Cartier, Impact ionization and degradation in silicon dioxide films on silicon, in: C.R. Helms, B.E. Deal (Eds.), The Physics and Chemistry of SiO_2 and the Si–SiO_2 Interface, vol. 2, Plenum Press, New York, 1993.
[16] P. Riedler, D. Morgan, Analysis of Irradiated and Annealed ATLAS Prototype Silicon Detectors, ATLAS Internal note INDET-No-209, 16.06.1998.
[17] S. Gadomski, P. Weilhammer, Nucl. Instr. and Meth. A 351 (1994) 201.
[18] R. Wunstorf, Systematische Untersuchungen zur Strahlenresistenz von Silizium-Detektoren für die Verwendung in Hochenergiephysik-Experimenten, Ph.D. Thesis, Universität Hamburg, 1992.